Delta J. Sci. 2010: 1-24 **Geology**

MINERALOGICAL, GEOCHEMICAL AND RADIOACTIVE ASPECTS OF NUWEIBI BASEMENT ROCKS, CENTRAL EASTERN DESERT, EGYPT.

Salah S. El-Balakssy, Mohamed A.Wetait* and Sameh M. Mansour
Nuclear Materials Authority, P.O. Box, 530, El Maadi, Cairo, Egypt.
*Geology Dept., Fac. Sciences, Benha Univ., Egypt.

e-mail; Salah_elbalakssy@ yahoo.com

(Received: 20-1-2010)

ABSTRACT: Nuweibi area is situated in the Central Eastern Desert, Egypt, covers an area of about 135 km^2. The field observations and the detailed petrographic study revealed that the mapped area is distinguished into several rock units: serpentinites, metasediments, metagabbros and older granites that intruded by albitized granites. The radiometric analyses revealed that the studied rocks exhibit low radioactive levels except for the albitized granites that can be attains relatively moderate eU and eTh contents. The radioactivity of Nuweibi albitized granites may be attributed to the dominance of thorite and some thorium bearing minerals as monazite and uranothorite, moreover, very scarcely grains of secondary uranium minerals as uranophane, autunite and chernikovite. Furthermore, zircon was documented as free grains or as inclusions within crystals lattice of cassiterite, garnet and titanite. Meanwhile, REE signatures are prevalence in allanite, chevkinite, fluorite, zircon, monazite, apatite and manganocoltan giving rise as a potential source for the REE in theses minerals. On the other hand, columbite, tantalite, tapiolite, and cassiterite are dominant as a rare-metal mineralization (Nb, Ta and Sn).

The taxopiokilitic texture as well as the prismatic bipyramidal zircon is a strong evidence for the magmatic origin of Nuweibi granite. Unlike the albitization processes give an idea about the Nuweibi granite may have been underwent an extensive hydrothermal alteration mainly Na-metasomatism. In addition to, the presence of characteristic variety of zircon such as mud zircon, as well as columbite, cassiterite, garnet, fluorite and apatite confirming the multistage of hydrothermal metasomatic origin. The significant enrichment of some trace elements in Nuweibi granites during the alteration could be attributed to the existence of some resistant and economic minerals in the study area.

Keywords: mineralogy, radioactivity, Nuweibi, basement rocks, Eastern Desert, Egypt.

INTRODUCTION

Nuweibi area is situated in the Central Eastern Desert, 30 km north of Marsa Alam and about 33 km west of the Red Sea coast. It is delineated by latitudes 25° 10' 30" and 25° 15' 15" N and longitudes 34° 29' 00" and 34° 38' 29" E, covering an area of about 135 km^2 (Fig.1). The area is mainly built up of metamorphic and igneous rocks of late Precambrian age represented by serpentinites, metasediments, metagabbros, older granites, albitized granites and post granite dykes.

Nuweibi area is previously studied by many authors, e.g Amin *et al.*, (1952); Awad, (1973); Sabet and Tsogoev, (1973); Sabet *et al.*, (1973&1976); Sabet, (1980); Geological Survey of Egypt, (1974); Riad, (1979); El Tabaal, (1980); Kamel and El-Tabbal, (1980); Naim *et al.*, (1996); Arslan,(1997); Helba *et al.*, (1997); Abu El-Maaty and Khalil, (1999 a&b); Abu El-Maaty and Ali Bik,(2000); Ghoneim,(2003); Abd El-Wahed,(2004) and Abdalla *et al.*, (2008). On the other hand, the present study essentially throws some light on the petrography, radioactivity, mineralogy and geochemistry of the albitized granites in Nuweibi area to clarify the uniqueness aspects of these rocks.

Sampling and analytical techniques

To achieve the preceding goals twenty representative samples were collected; three from each of the serpentinites, metasediments, metagabbroic rocks and older granites were selected for whole rocks study (Fig.1) beside, eight samples from albitized granites (Fig.2). The following investigations were carried out on the studied area, Firstly, thin sections represent the examined rocks were prepared for petrographical studies. Secondly, detailed aeroradiometrical maps of study area were prepared from airborne gamma-ray spectrometry survey data, beside the ground radiometric analyses were carried out by Gamma-ray spectrometry multichannel analyzer techniques. The mineralogical studies were carefully investigated using heavy liquid separations and magnetic fractionation followed by microscopic examinations.

The recorded minerals were verified by Environmental Scanning Electron Microscope (ESEM) model Philips (XL, 30) and the X-ray diffraction analysis (XRD). The major oxides were measured for eight albitized granite samples using the wet chemical techniques (Shapiro and Brannock, 1962) while the trace elements were determined by XRF. All analyses were done in the Nuclear Materials Authority (NMA) Labs., Egypt.

Geologic setting:

Metasediments have wide exposures at the eastern, northern and southern sectors of the studied area. They are dissected by dykes and cassiterite-bearing quartz veins. They represented by, quartz biotite schist, quartz feldspar biotite schist and quartz biotite amphibole schist (Riad 1979).

Serpentinites occur as a small lensoidal and irregular bodies either cutting the metasediments or captured by the older granites. The serpentinites resulted from a low temperature metasomatic alteration of pre-existing peridotite. Some serpentinites transformed later to talc. It is consists of antigorite and talc after olivine and pyroxene.

Metagabbros, hornblende metagabbros constitute the entire south eastern part of the Nuweibi area. Their intrusive contacts with the schists steeply westward. The metagabbros are medium-grained rocks and in some relatively fine-grained with zones of microgabbros.

Older granites outcrop in the north and the south of the albite granite massif. They show sharp contacts against schists, metagabbro and are intruded by albite granites. It is grey in color, fine to medium-grained. It is composed essentially of feldspars, quartz and biotite. It comprises granodiorites and tonalite.

Albitized granite massif was developed through high temperature multistage metasomatism and belonged to final stage of the Gattarian intrusive (Sabet *et al.*, 1973 and El Tabaal, 1980). This granite appears to be formed along the fault plane of N-S direction which in turn divides the massif into two main blocks (Riad, 1979). It displays intermediate position between normal and subalkaline albite granite (Sabet, 1980). This granite crystallized through four steps, considered as A-type granites that were emplaced at high crustal levels. (Helba *et al.*, 1997 and Abu El-Maaty and Ali Bik, 2000).

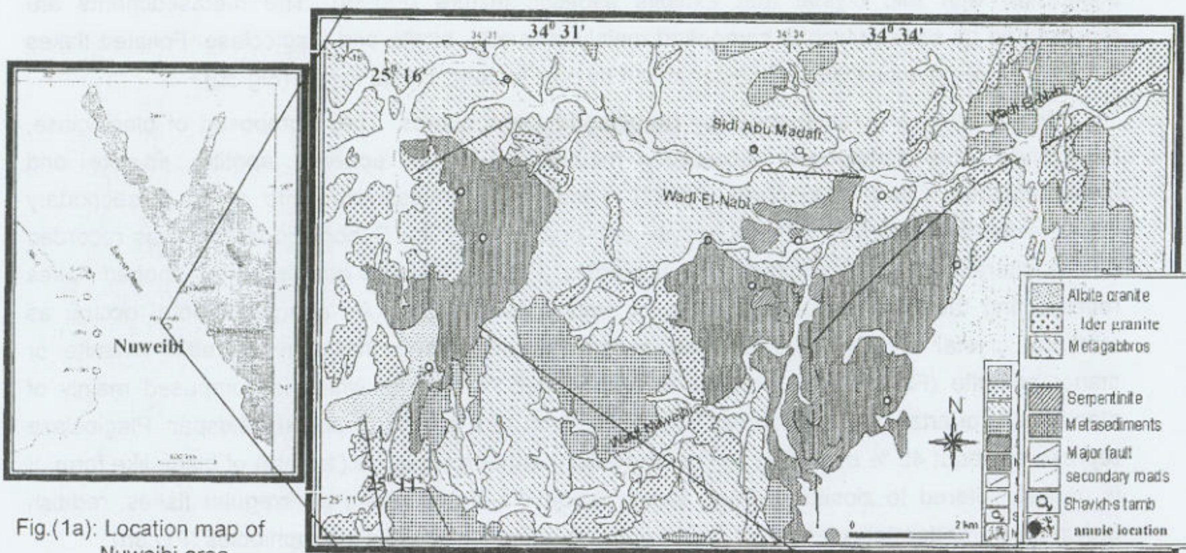

Fig.(1a): Location map of Nuweibi area

Fig. (1 b): Geological map of Nuweibi area (after geological survey of Egypt, 1991)

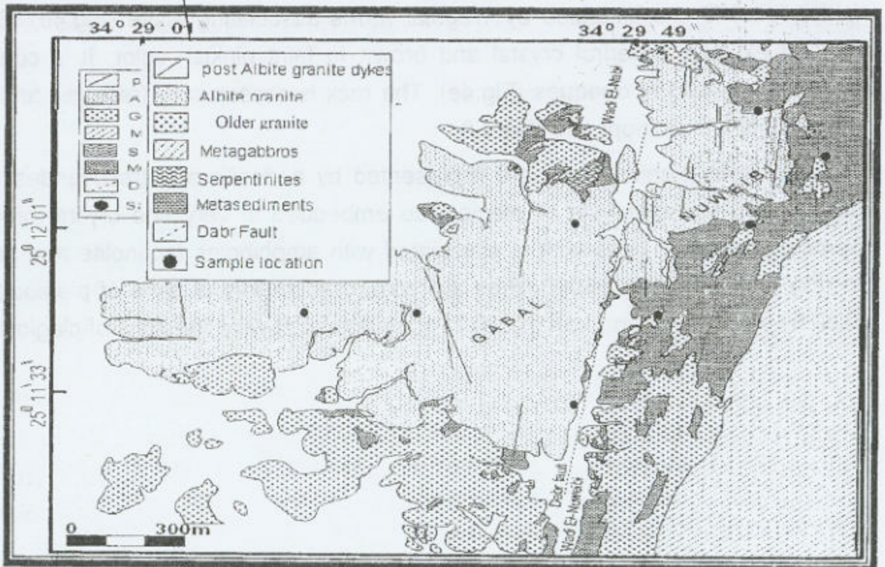

Fig. (2): Details geological map for albitized granites from Nuweibi area.(after Helba *et al.*, 1997)

Petrographical investigation

The characteristic petrographical features of the different rock units encountered in the study area revealed that serpentinites is composed of serpentine minerals, mainly platy crystals of antigorite associated with talc crystal that exhibits asbestic texture (Fig.3a). The metasediments are represented by schist which is composed mainly of quartz, biotite and plagioclase. Foliated flakes of biotite showing schistosity (syntectonic) cut by post tectonic biotite flakes (Fig.3b).

Metagabbros are represented by hornblende metagabbros. They composed of plagioclase, hornblende and biotite with accessory minerals such as sphene, apatite, epidote and titanomagnetite. Calcic-plagioclase (An-62) is intensively saussuritized into group of secondary minerals as carbonate, sericite, muscovite and epidote (Fig.3c). Subophitic texture was recorded due to alteration of clinopyroxene to amphiboles (Fig.3d). Chlorite occurs as fan-shaped flakes representing the end alteration product of amphiboles (Fig.3e). An opaque mineral occurs as anhedral crystal of magnetite mantled by sphene suggesting that may be after ilmenite or titanomagnetite (Fig.3f). Older granite is represented by tonalite which is composed mainly of plagioclase, quartz, rare amphiboles and biotite with rare crystal of potash feldspar. Plagioclase represents about 45 % occurring as fine-to medium euhedral crystals (1.3mm) of blade like form. It is partially altered to ziosite (Fig.3g). Biotite (about 15 %) occurring as irregular flakes, reddish brown color, moderately pleochroic and may be an alteration product of amphiboles (Fig.3h)

Albite granite is composed of albite, quartz, microcline and mica with accessory minerals as sphene, garnet and fluorite. Albite represents about 65 % of the rock. It occurs as coarse subhedral crystals and as fine anhedral crystals associated with perthite that included in quartz forming taxopiokilitic texture (snow ball texture) as shown in Figure (4a). This texture revealed the magmatic origin and indicates the co-precipitation of quartz and albite from a progressively fractionating Na- rich melt (Abdalla *et al.*, 1998 & 2008 and Abdalla & Mohamed, 1999). Unlike, the presence of albite is mainly related to albitization or Na- metasomatism indicating an extensive hydrothermal alteration, therefore, two phases of formations could be occurred. Potash feldspar occurs as subhedral microcline crystals or as anhedral perthite crystals enclosed in quartz crystals (Fig.4b). Also, presence of antiperthite which surrounded by fractured plagioclase (Fig.4c). Mica (phlogobite) is characterized by irregular forms associating albite (Fig.4d). Sphene as accessory mineral exhibits anhedral crystal and brown to faint pinkish color. It is considered as the main alteration product of opaques (Fig.4e). The rock is occasionally fractured and filled with iron oxide associated with uranophane (Fig.4 f).

The post granite dykes are represented by andesite and trachyandesite dykes. Andesite is composed of phenocrysts of plagioclase embedded in very fine crystal of andesine plagioclase forming porphyritic texture. It is associated with amphiboles (actinolite and hornblende) as shown in (Fig. 4g). Trachyandesite dykes are composed mainly of laths of plagioclase showing veinlete filled by chalcedony and iron oxides in groundmass of very fine laths of plagioclase (Fig.4 h).

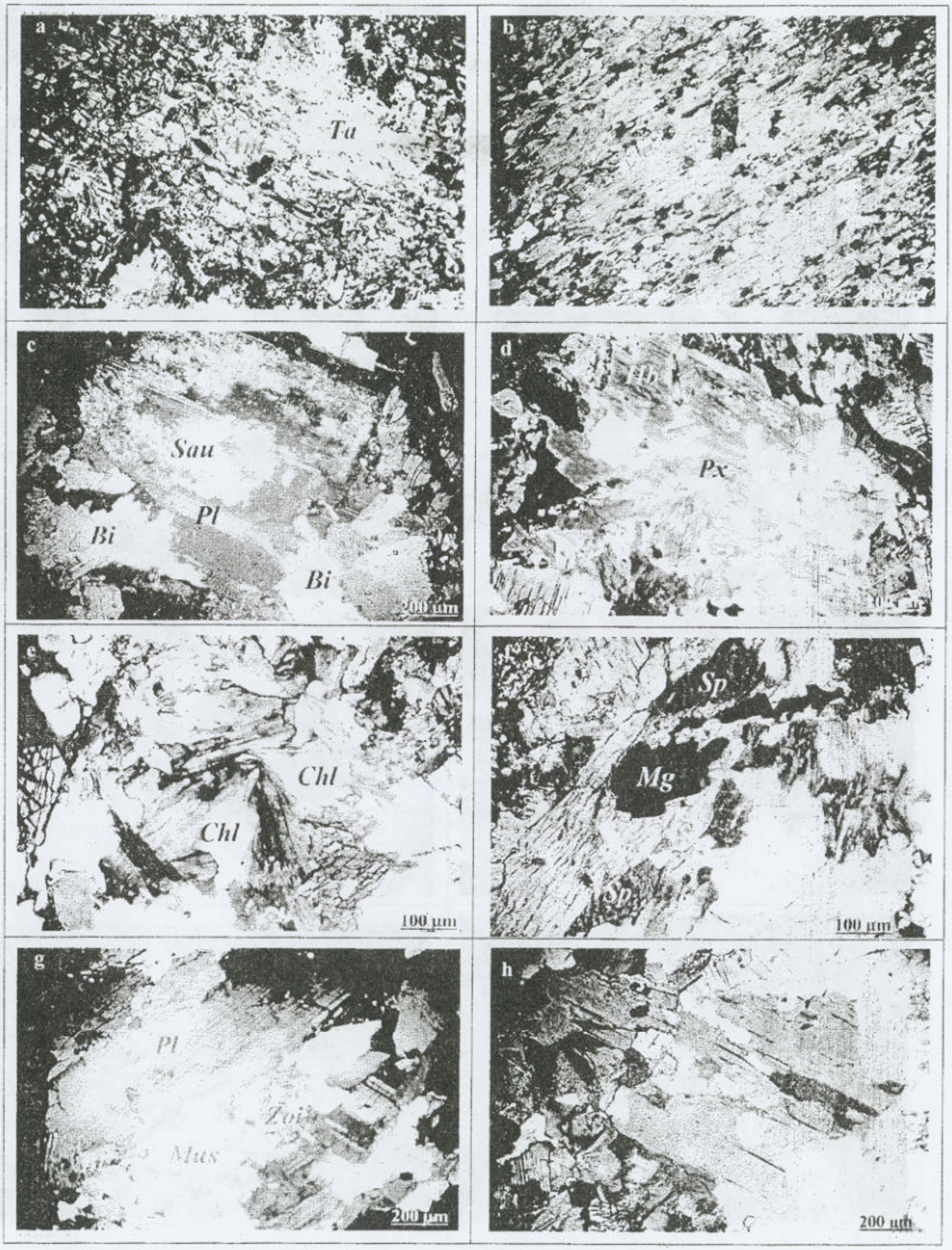

Fig. (3): Photomicrographs of Nuweibi basement rocks showing: C. N.
a): Talc (*Ta*) showing asbestic texture associating platy crystals of antigorite (*Ant*) in serpentinites.
b): Foliated flakes of biotite showing schistosity (syntectonic) cut by post tectonic biotite flakes in metasedimentary rocks.
c): Saussuritization (*Sau*) of calcic plagioclase (*PL*) associating biotite (*BI*) in metagabbros.
d): Mega crystal of hornblende (*Hb*) after clinopyroxene (*Px*) forming subophitic texture in metagabbros.
e): Fan-shaped chlorite (*Chl*) in metagabbros.
f): Magnetite (*Mg*) mantled by sphene (*Sp*) in metagabbros.
g): Alteration of plagioclase (*Pl*) to zoisite (*ZOI*) and biotite (*Bi*) partially altered to muscovite in older granites.
h): Amphibole (*Am*) associated with biotite (B*i*) in older granites.

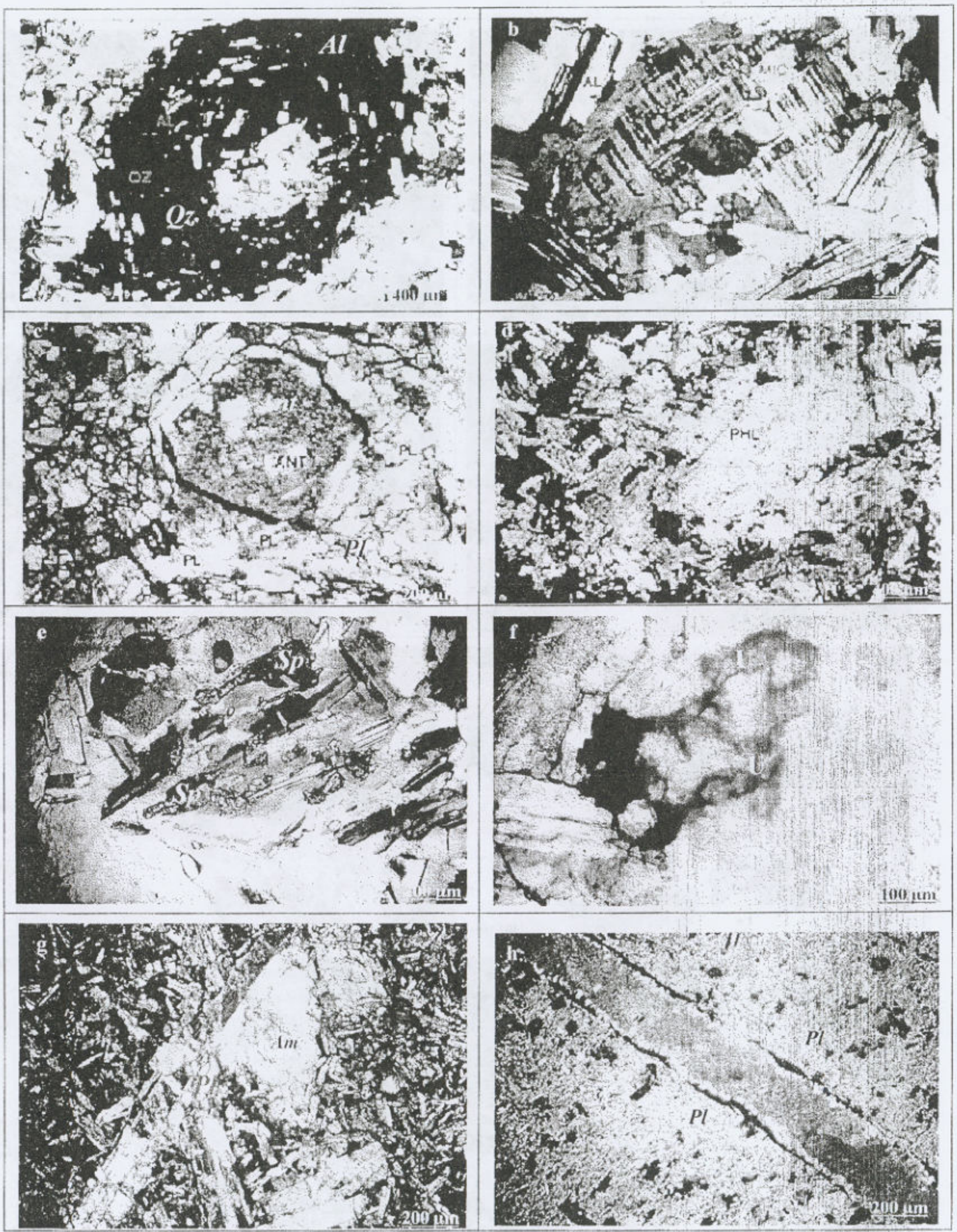

Fig. (4): Photomicrographs *of albitized granites showing:*

a): Quartz (*Qz*) including fine crystals of albite (*Al*) with perthite showing taxopoikilitic texture. C. N.

b): Discrete laths of albite (Al) surrounding potash feldspar mainly microcline (Mic). C. N.

c): Antiperthite (*Ant*) surrounded by fractured plagioclase (*Pl*). p.p.L

d): Secondary flake of phlogobite (*Phl*) associating with albite. C. N.

e): Sphene (*Sp*) as accessory mineral in albitized granites. C. N.

f): Fractures filled with iron oxide associated with radioactive materials may be uranophane (U). p.p.L.

g): Phenocrysts of plagioclase (*Pl*) associated with fresh amphibole (*Am*). C. N.

h): A veinlete filled by chalcedony and iron oxides in groundmass of laths of plagioclase (*Pl*). C. N.

Radioactivity and their distributions in rock exposures

Different collaborative radiometric techniques such as aeroradiometric survey and ground radiometry were adopted. Firstly, the present work deals with the analysis and interpretation of airborne gamma-ray spectrometric of Nuweibi area that had been carried out by Aero Service Division, Western Geophysical Company of America in 1984. Accordingly, Radioelements contour maps (eU_{ppm}, eTh_{ppm} and K %) as well as total count (μr) has been constructed. They are superimposed on the geological map of the area (Figs.5a, 5b, 5c & 5d) to identify the most radioactive localities in the study area as promising for potential radioactive sources. Hence, the distribution of the three radioelements (eU_{ppm}, eTh_{ppm} and K %), beside the total count (μr) of Nuweibi basement rocks were determined. The resulted data were summarized in Table (1).

The total count map of Nuweibi area revealed that, the contour line values of 22 μr are mainly associated with metagabbro which apparently exhibits low radiometric values while granites exhibit superimposed contour lines and display three specific trends (NNE-SSW, NW-SE and E-W). Generally, granites are carefully delineated by total-count level of 42 μr. Accordingly, the obtained radiometric maps revealed that the serpentinites, metasediments, metagabbros and older granites show low contents of eU ranging from 0.85 to 1.62 ppm, eTh vary from 1.59 to 1.88 ppm and K ranging from 0.61 to 1.21%. On the other hand, the albitized granites have a moderate radioactive level. It is in the range of 1.80 to 2.92 ppm for eU, from 5.19 to 11.61 ppm for eTh and from1.38 to 1.95 % for K. These results are consistence with Ali (2003) reported that the ultramafic rocks attain lowest radioactivity (1.4 μr) while the highest one in siliceous rocks.

Furthermore, in order to define the trends of uranium migration, the uranium migration eU-(eTh/3.5) ratio contour map (Fig. 5e) was illustrated taking in consideration the negative contours represent the leaching-out while the positive contours indicate the leaching-in (albitized granites). Also, vector map were constructed (Fig. 5f) revealed that, in the eastern side; uranium leached from albitized granites towards the country rocks which represented by schist and metagabbros while in the western side, uranium leached out from the albitized granites and grey granites towards the contact in between may be due to the presence of fault plane of N-S direction. Consequently, the western part of the studied albitized granites generally exhibits distinctly high radioactive level than do other parts.

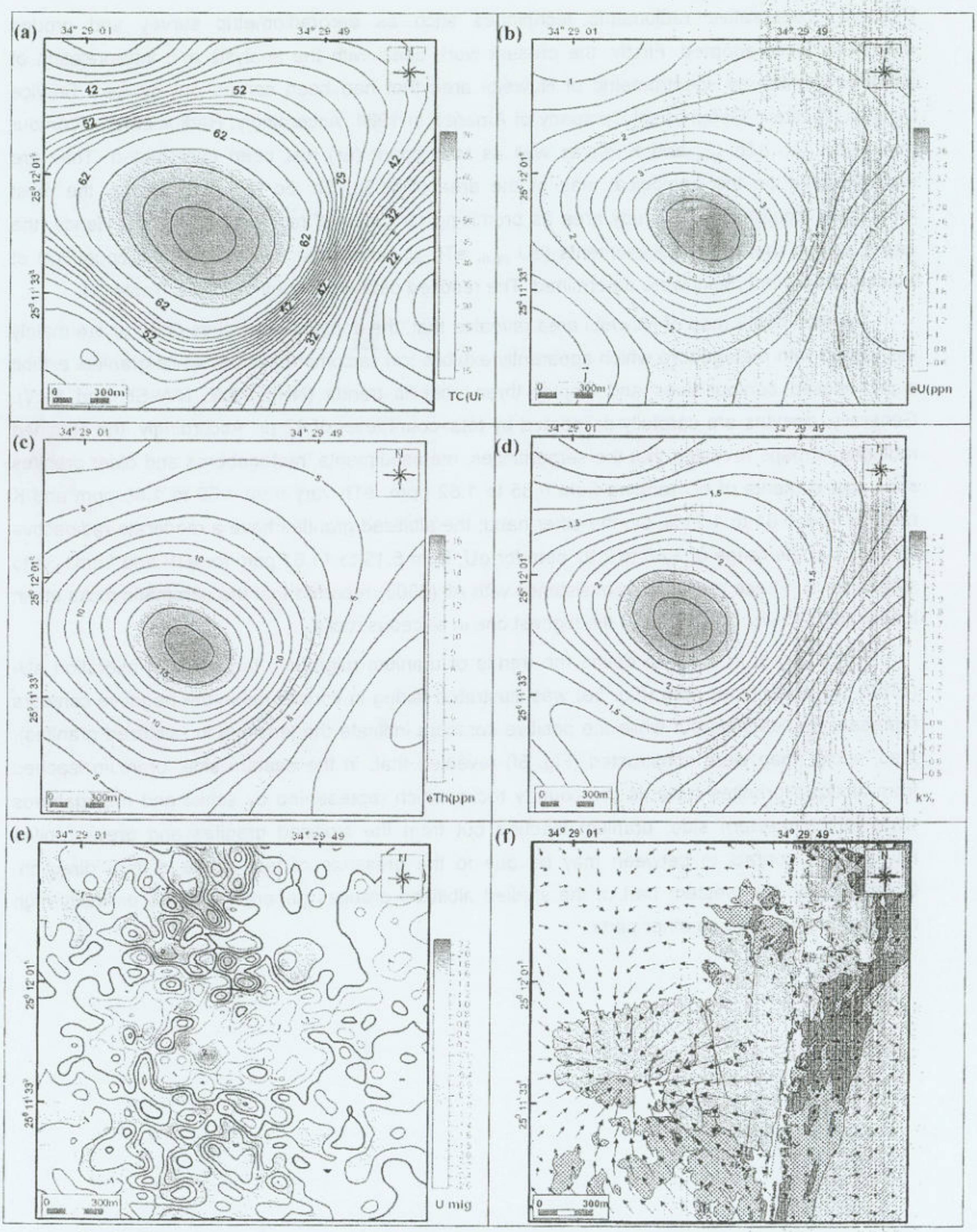

Fig. (5): Airborne radioactive contour maps of Nuweibi area.
(a) Total-count (μr) (b) Equivalent uranium (ppm)
(c) Equivalent thorium (ppm) (d) Potassium (%)
(e) Uranium migration contour map (f) Uranium migration vector map μr: unit of radioelement concentration
(1.0 ppm eU = 1.0 μr = 0.6 μR/h) (1.0 ppm eTh = 0.5 μr = 0.2 μR/hr) (1.0 % K = 2.6 μr = 1.18 μR/hr)

Table (1): Average airborne gamma-ray spectrometric data for Nuweibi area.

Rock units	Elements	Min.	Max.	Av.
Albitized granites (Western side) N=171	eU	1.45	3.93	2.92
	eTh	4.37	18.80	11.61
	K	1.02	2.46	1.95
	T.C	40.60	70.90	64.38
Albitized granites (Eastern side) N= 52	eU	1.39	2.30	1.80
	eTh	4.50	6.75	5.19
	K	1.23	1.58	1.38
	T.C	43.50	58.70	48.60
Grey granites N= 115	eU	0.81	2.34	1.62
	eTh	1.70	2.84	1.88
	K	0.67	2.05	1.21
	T.C	23.30	64.20	44.14
Metagabbros N= 107	eU	0.50	1.35	0.85
	eTh	0.62	2.56	1.65
	K	0.46	0.99	0.61
	T.C	13.20	34.20	20.39
Metasediments N= 99	eU	1.01	1.61	1.38
	eTh	1.78	1.89	1.59
	K	0.69	1.70	1.16
	T.C	24.50	62.40	41.66

N = total number of measurements

On the other hand, the concentrations of the four radioelements (eU, eTh, eRa and K %) were estimated in the western part of Nuweibi albitized granite using Gamma-ray spectrometry multichannel analyzer techniques (Table 2). The obtained data show that eU contents vary from 7 to17 ppm with an average of 10 ppm while eTh contents range from 13 to 26 ppm with an average of 21 ppm. The eTh/eU ratio ranges from 1.06 to 3.25 with an average of 2.10 which is lower than the standard value of granitic rocks (eTh/eU= 3.5-3.8) that was given by Cambon (1994), revealing uranium enrichment relative to thorium content. The eRa is about 5 ppm while the k content varies from 2.03 to 3.40 % with an average of about 2.63 %.

Table (2): Gamma-ray spectrometry multichannel analyzer of albitized granites

	Sample No.	eU (ppm)	eTh (ppm)	eRa (ppm)	K (%)	eTh/eU
Eastern part	1	9	22	5	2.62	2.44
	2	7	13	5	2.03	1.86
	3	7	20	5	2.28	2.86
Western part	4	10	24	5	2.84	2.40
	5	11	19	5	2.79	1.73
	6	8	26	5	3.40	3.25
	7	17	18	5	2.48	1.06
	8	9	20	5	2.62	2.22
	Av.	10	21	5	2.63	2.10

Moreover, weakly positive relation between eU and eTh (r= 0.14), the eTh and eTh/eU ratio show strongly positive relation (r=0.73), while moderately negative relation between eU and eTh/eU ratio (r=-0.56) were recorded and revealing the post-magmatic processes that controlled the uranium enrichment in studied albitized granites (Figs.6a, b&c).

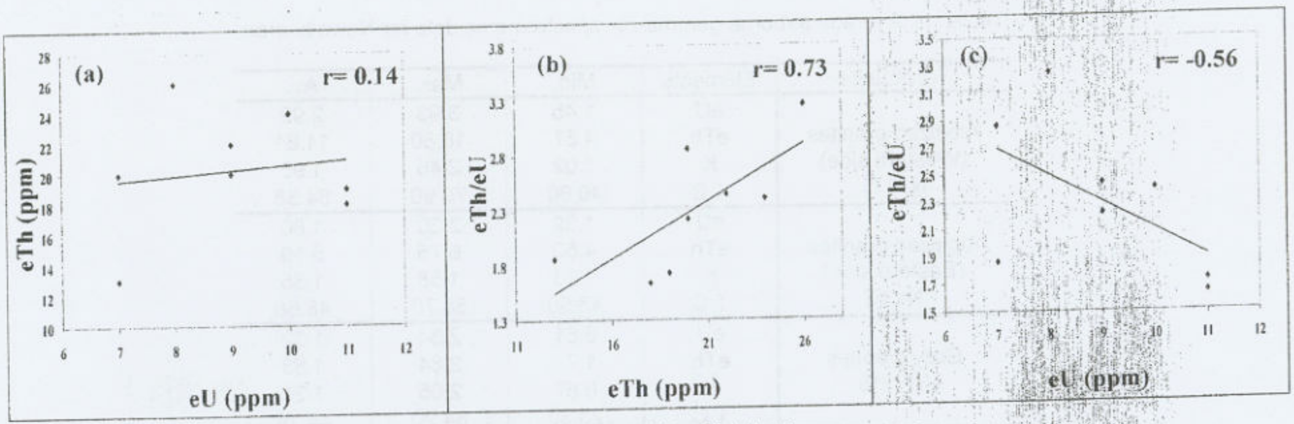

Fig.(6): Relations of eU Vs eTh ; eTh Vs eTh/eU ratio and eU Vs eTh/eU ratio.

Accordingly, due to the relative moderate radioactivity was recorded only in the albitized granite rocks, therefore, it is necessary to investigate their mineralogical composition and their chemical characteristics to verify the minerals that responsible for the radioactivity of this pluton as well as their economic importance.

Mineralogical investigation of Nuweibi albitized granites

The mineralogical investigation of Nuweibi albitized granites reveals the dominance of various rare-metals and radioactive accessory minerals.

I- Rare-metal bearing minerals (Nb, Ta & Sn)

1.1. Niobium and tantalum series

Columbite $(Fe,Mn)(Nb,Ta)_2O_6$ and tantalite $(Fe,Mn)(Ta,Nb)_2O_6$ are the most niobates and tantalates occurs. They were recorded as, flattened, stubby, smooth surface, fine sand size crystal or aggregates, vary in color from reddish brown to dark black, and exhibits weak magnetism. ESEM microanalysis revealed the presence of characteristic variety of these minerals. Both minerals have short prismatic (Fig.7) with the same crystal habit (orthorhombic). Therefore, they display isomorphism phenomenon, the solid solution depending on the Nb and Ta percentages, beside the iron and manganese contents vary considerably.

On the other hand, some tantalum-rich grains attains tetragonal habit revealed the presence of tapiolite mineral (Fe, Mn) $(Ta, Nb)_2$ O_6 that makes polymorphism with tantalite (Fig.8). The tapiolite mineral is characteristic variety for albitized granites (Kraus, *et al.*, 1951). The columbite and tantalite mixture is called coltan ore. The REE bearing manganocoltan grain {$Mn (Nb, Ta)_2 O_6$} was shown in (Fig.9). Generally, niobium and zircon mineralization have close paragenetic association with the albitization. Niobium containing granites described as a metasomatic and derived by intensive albitization and rare-metal metasomatism (Severov, 1963).

1.2. Cassiterite (SnO_2)

Cassiterite is another rare metal in the studied granites. They exhibits fine and very fine sand size, subangular to subrounded, massive, thin acicular needles or short prismatic, vary in color from black, brown to red. Some grains shows euhedral outlines. The ESEM revealed the presence of different cassiterite habits (Fig.10).

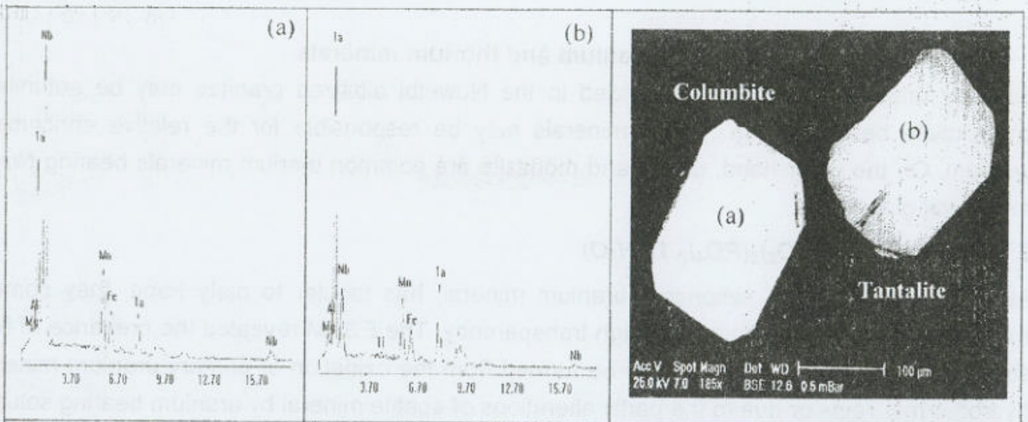

Fig. (7): EDX and BSE image showing stubby crystals of columbite (a) and tantalite (b).

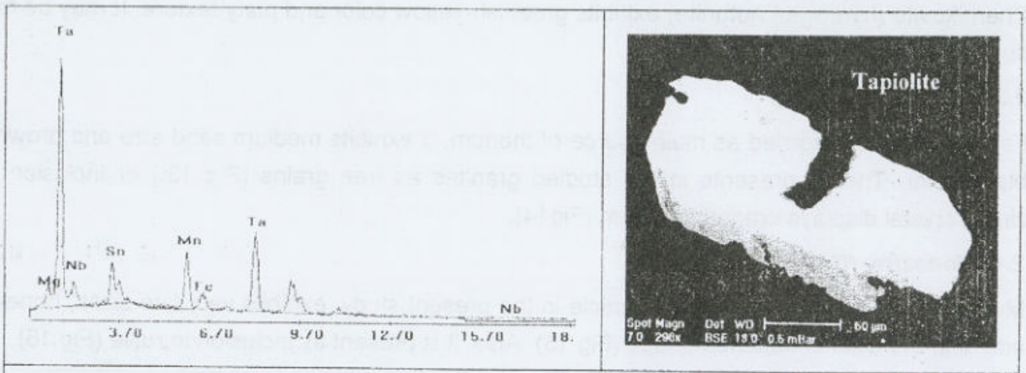

Fig. (8): EDX and BSE image showing tetragonal tapiolite grain.

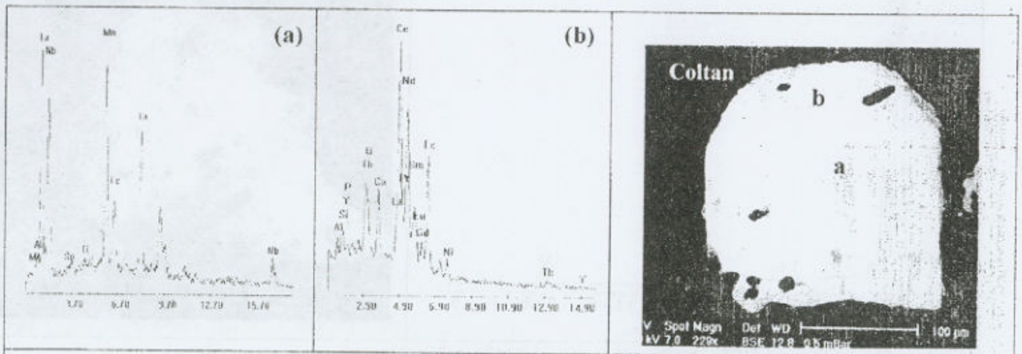

Fig. (9): EDX and BSE image showing mangano coltan grain (a) exhibits REE (b).

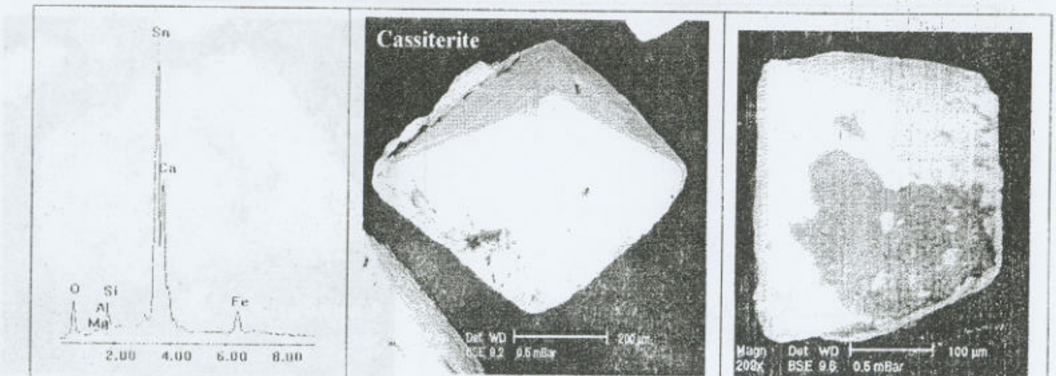

Fig. (10): EDX and BSE image showing different cassiterite habits.

2-Uranium and thorium minerals

Scarcely uranium grains were recorded in the Nuweibi albitized granites may be autunite and chernikovite beside, zircon. These minerals may be responsible for the relative enrichment of uranium. On the other hand, thorite and monazite are common thorium minerals bearing Nuweibi-rare metal granites.

2.1 Autunite Ca $(UO_2)_2(PO_4)_2.12(H_2O)$

Autunite considered as secondary uranium mineral, has tabular to platy habit, they commonly exhibits yellowish green color with high transparency. The ESEM revealed the presence of fibrous structure of autunite (Fig.11). It may be formed from the oxidation of primary uranium minerals in hydrothermal veins or due to the partly alterations of apatite mineral by uranium bearing solution.

2.2. Chernikovite $(H_3O)_2(UO_2)_2(PO_4)_2.6(H_2O)$

Chernikovite (hydrogen autunite) exhibits greenish-yellow color and platy texture. It may be formed due to oxidation of autunite (Fig.12).

2.3. Thorite (Th SiO_4)

Ferrithorite was recorded as main source of thorium. It exhibits medium sand size and brownish to black color. Thorite presents in the studied granites as free grains (Fig 13.) or inclusion within zircon crystal displays uranothirite form (Fig14).

2.4. Monazite (Ce, Th, La, Y, PO_4)

Monazite was recorded as a free particle in the present study, exhibits very fine sizes, honey color and displays distinct flattened shape (Fig.15). Also, it is present as inclusion in rutile (Fig.16).

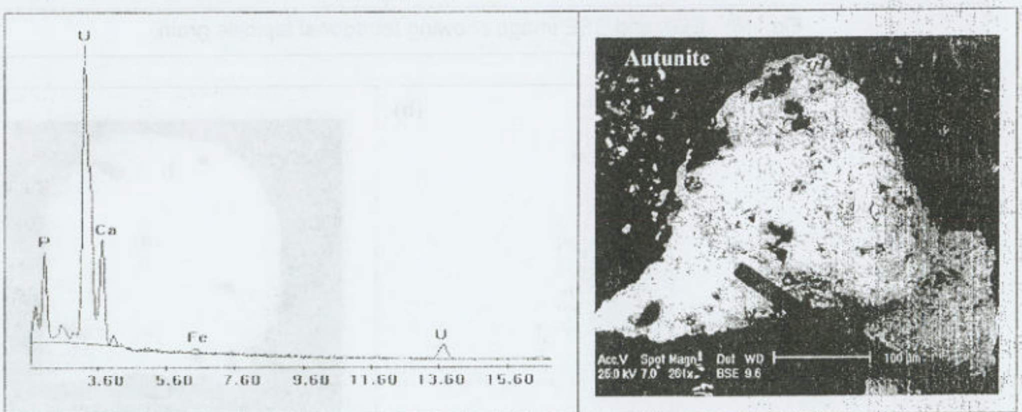

Fig. (11): EDX and BSE image showing autunite mineral.

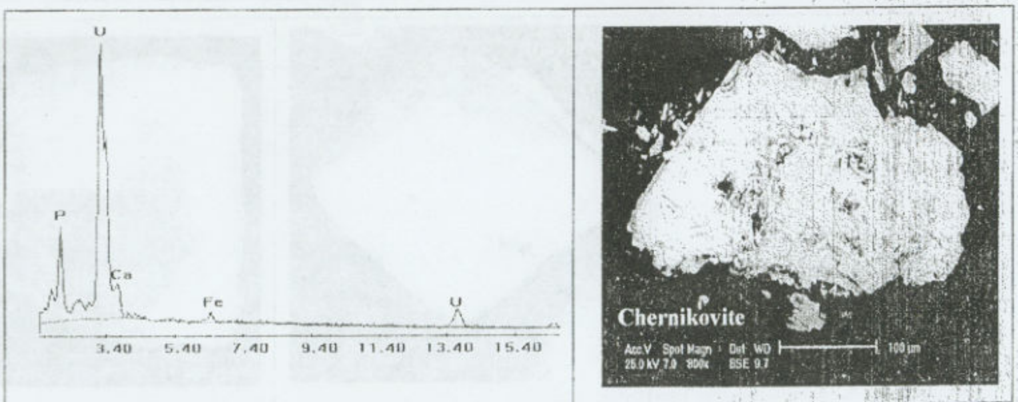

Fig. (12): EDX and BSE image showing chernikovite (hydrogen autunite) mineral.

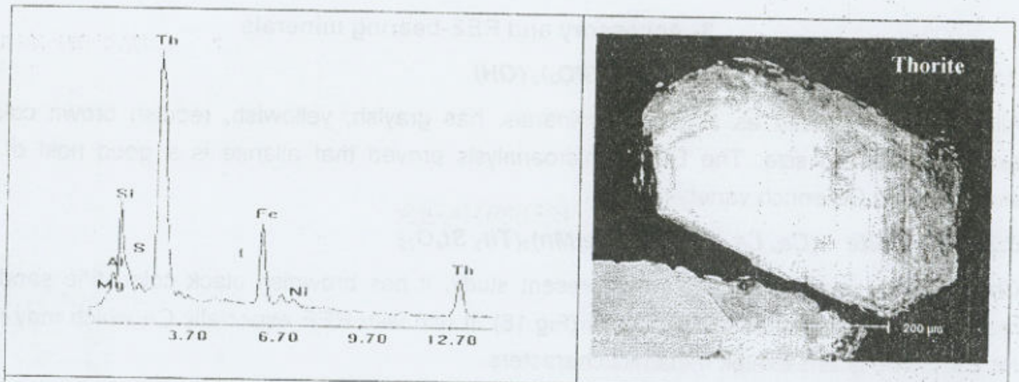

Fig. (13): EDX and BSE image showing ferrithorite mineral.

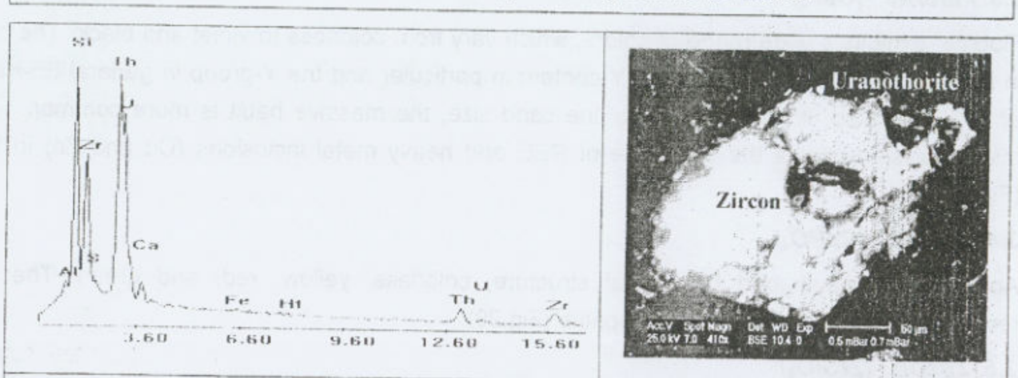

Fig. (14): EDX and BSE image showing uranothorite in zircon.

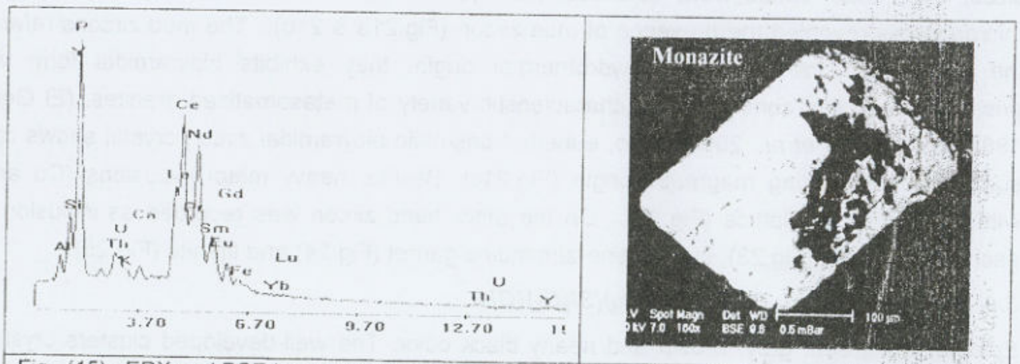

Fig. (15): EDX and BSE image showing pure monazite mineral.

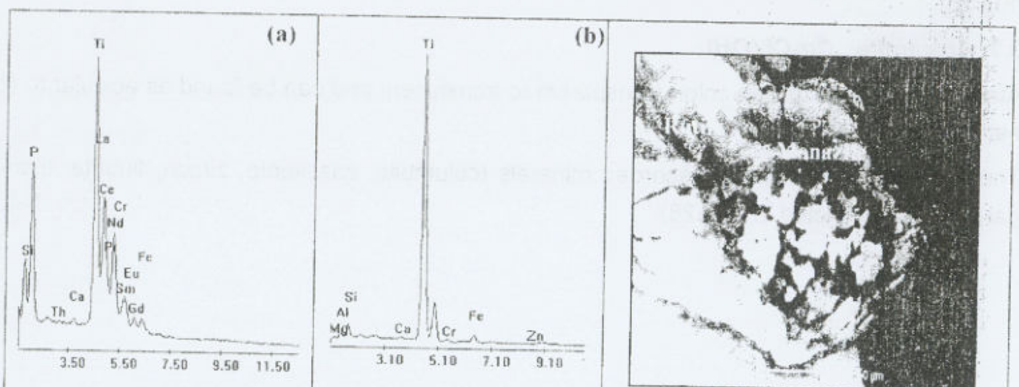

Fig. (16): EDX and BSE image showing monazite inclusion (a) in rutile (b).

3- Accessory and REE-bearing minerals

3.1. Allanite (Ce, Ca, Y)$_2$ (AL,Fe^{+3})$_3$(SiO$_4$)$_3$ (OH)

Allanite was recorded as accessory minerals, has grayish, yellowish, reddish brown color and exhibits fine sand size. The ESEM microanalysis proved that allanite is a good host of LREE especially the Ce-enrich variety (Fig.17).

3.2. Chevkinite (Ce, La, Ca, Th)$_4$ (Fe,Mn)$_2$(Ti)$_3$ Si$_4$O$_{22}$

Chevkinite is rarely recorded in the present study. It has brownish black color, fine sandy size, massive fragment or need-like crystals (Fig.18). It rich with REE especially Ce which may replace for Ca. Some grains exhibit metamict characters.

3.3. Fluorite (CaF$_2$)

Fluorite, exhibits a wide range of colors, which vary from colorless to violet and black. The change in fluorite color is controlled by the Y content in particular and the Y-group in general (El-Kammar *et al.* 1997) Also, it has medium to fine sand size, the massive habit is more common. ESEM microanalysis upholds the existence of REE and heavy metal inclusions (Cu and Zn) in fluorite (Fig.19).

3.4. Apatite (CaPO$_4$)

Apatite has well-shaped hexagonal structure, colorless, yellow, red, and green. The ESEM revealed the presence of REE rich apatite (Fig.20).

2.5. Zircon (ZrSiO$_4$)

Zircon was recorded as common accessory mineral in the albitized granites. It has different sand sizes; their color varies from colorless, pale yellow, reddish yellow and honey. The ESEM microanalysis revealed the presence of mud zircon (Fig.21a & 21b). The mud zircons referred as the metasomatic zircon mainly hydrothermal origin, they exhibits bipyramidal form without prismatic faces and considered as characteristic variety of metasomatized granites, (El Gemmizi, 1984 and Abdalla *et al.*, 2008). Also, euhedral prismatic bipyramidal zircon crystal shows cracked surface and indicating magmatic origin (Fig.21c). Beside, heavy metal inclusions (Cu and Zn) within zircon crystal lattice (Fig.22). On the other hand zircon was recorded as inclusion within each of cassiterite (Fig.23), spessartine-almandine garnet (Fig.24) and titanite (Fig.25).

3.6. Epidote Ca$_2$(Al, Fe) Al$_2$O(SiO$_4$)(Si$_2$O$_7$)(OH)

Epidote has green, grey, brown and nearly black color. The well-developed clusters crystals are common. ESEM revealed the presence of heavy metals inclusion (Cu and Zn) within epidote (Fig.26).

3.7. Atacamite Cu$_2$Cl (OH)$_3$

Atacamite has dark green color, transparent to translucent and can be found as acicular to fibrous habits (Fig.27).

The XRD patterns of some recorded minerals (columbite, cassiterite, zircon, fluorite, titanite and garnet) were depicted in (Fig.28).

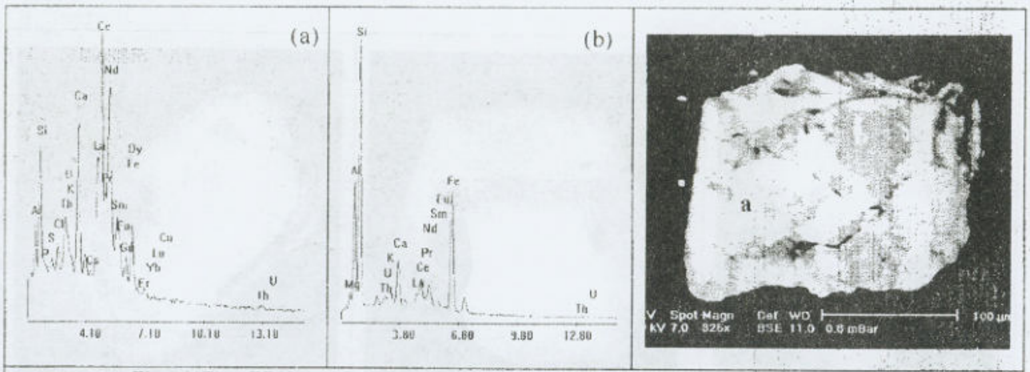

Fig. (17): EDX and BSE image showing highly REE (a) bearing allanite (b).

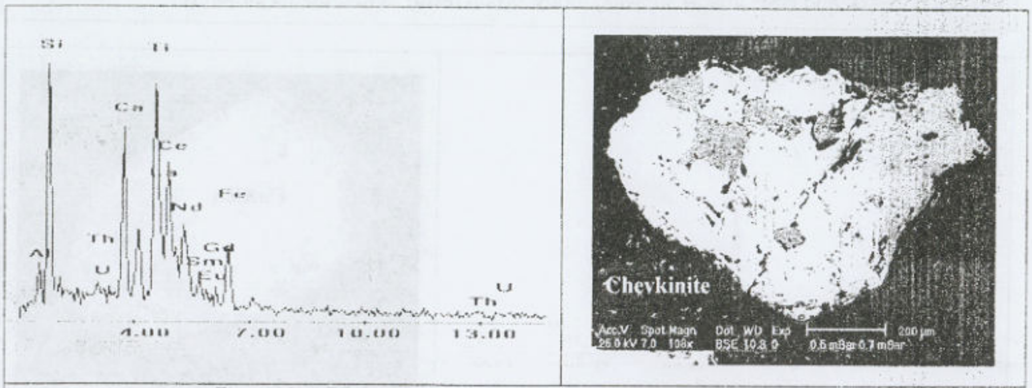

Fig. (18): EDX and BSE image showing chevkinite mineral.

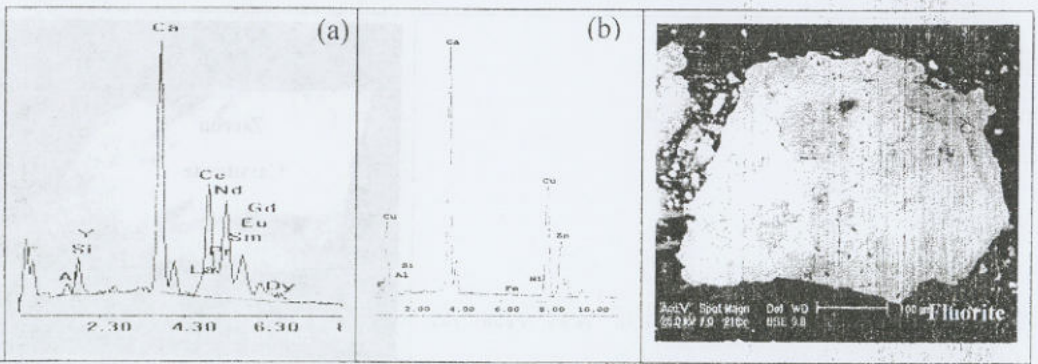

Fig. (19): EDX and BSE image showing REE (a) and heavy metal inclusions (b) in fluorite.

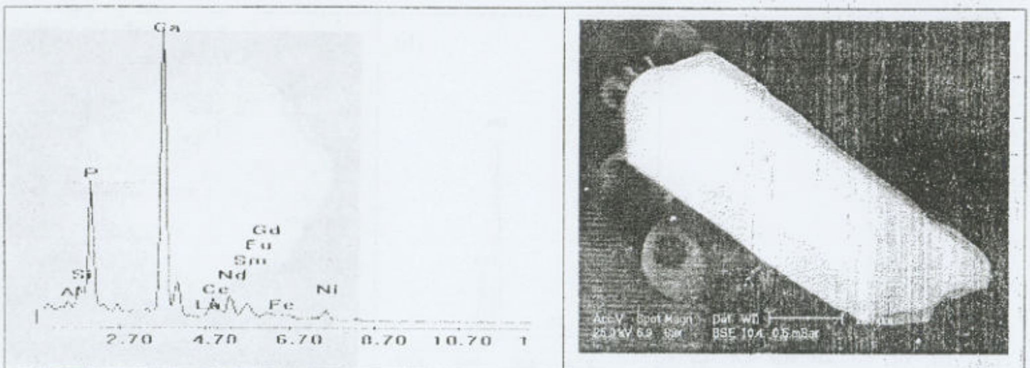

Fig. (20): EDX and BSE image showing REE rich apatite.

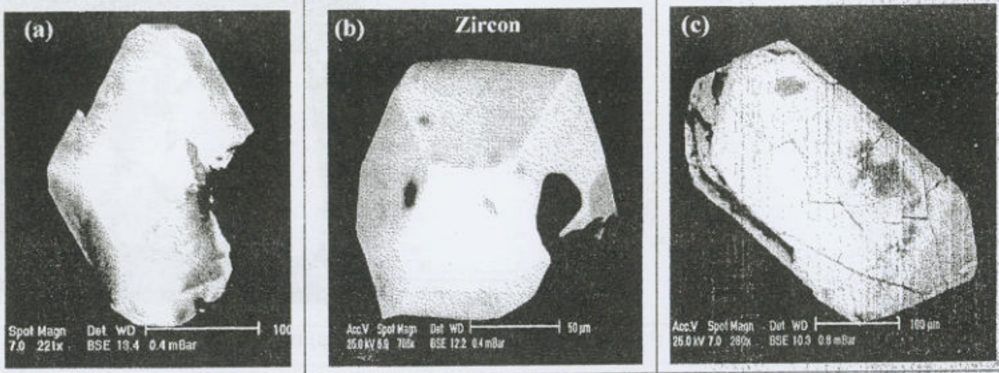

Fig. (21): EDX and BSE image showing mudy zircon (a&b) and cracked zircon (c)

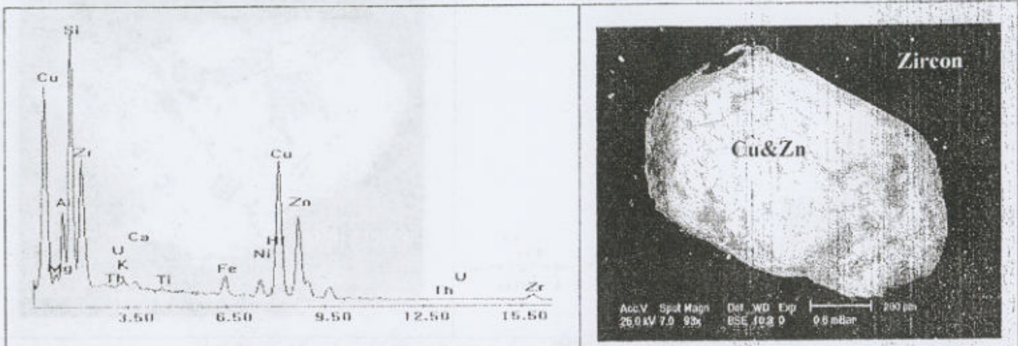

Fig. (22): EDX and BSE image showing heavy metal inclusions (Cu &Zn) in zircon.

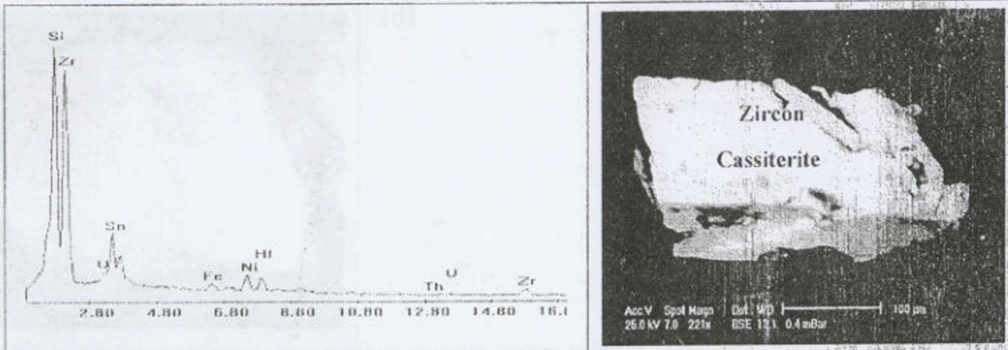

Fig. (23): EDX and BSE image showing zircon inclusion in cassiterite.

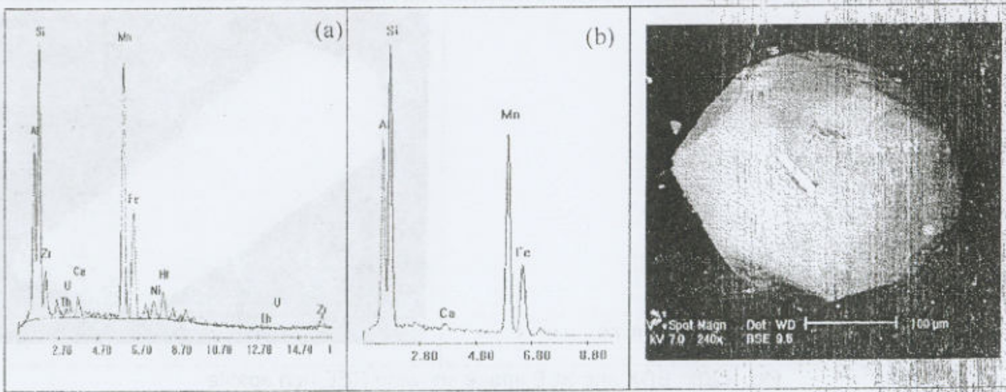

• Fig. (24): EDX and BSE image showing zircon inclusion (a) in garnet (b).

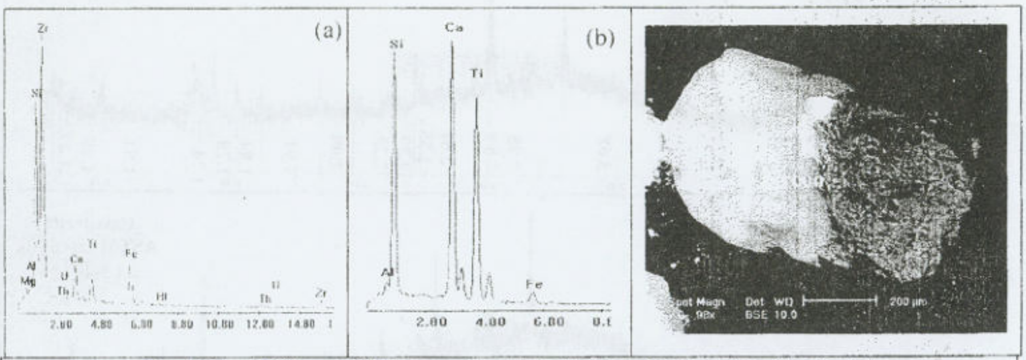

Fig. (25): EDX and BSE image showing zircon inclusion (a) in titanite (b).

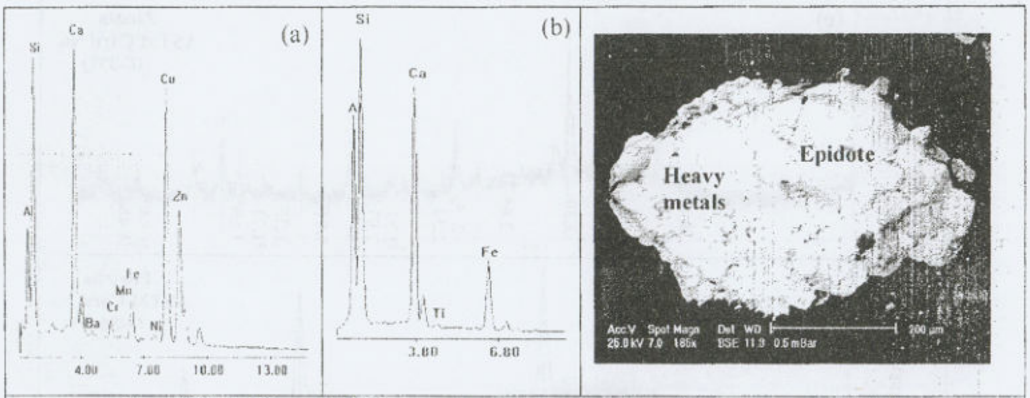

Fig. (26): EDX and BSE image showing heavy metals (a) bearing epidote (b).

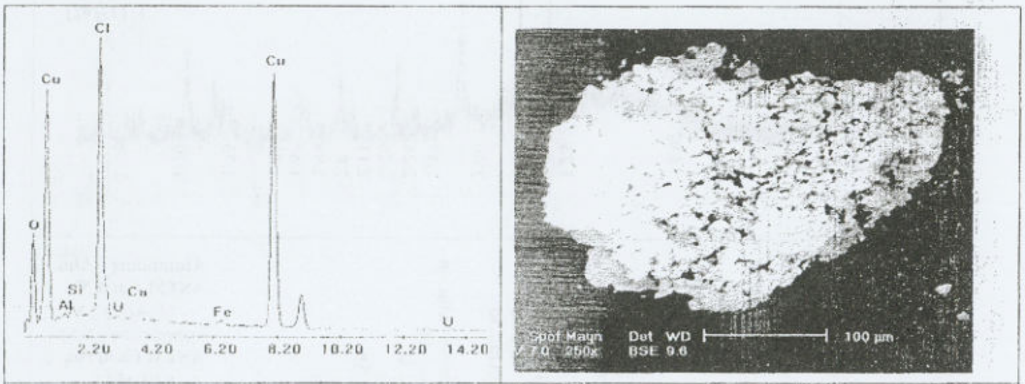

Fig. (27): EDX and BSE image showing atacamite grain.

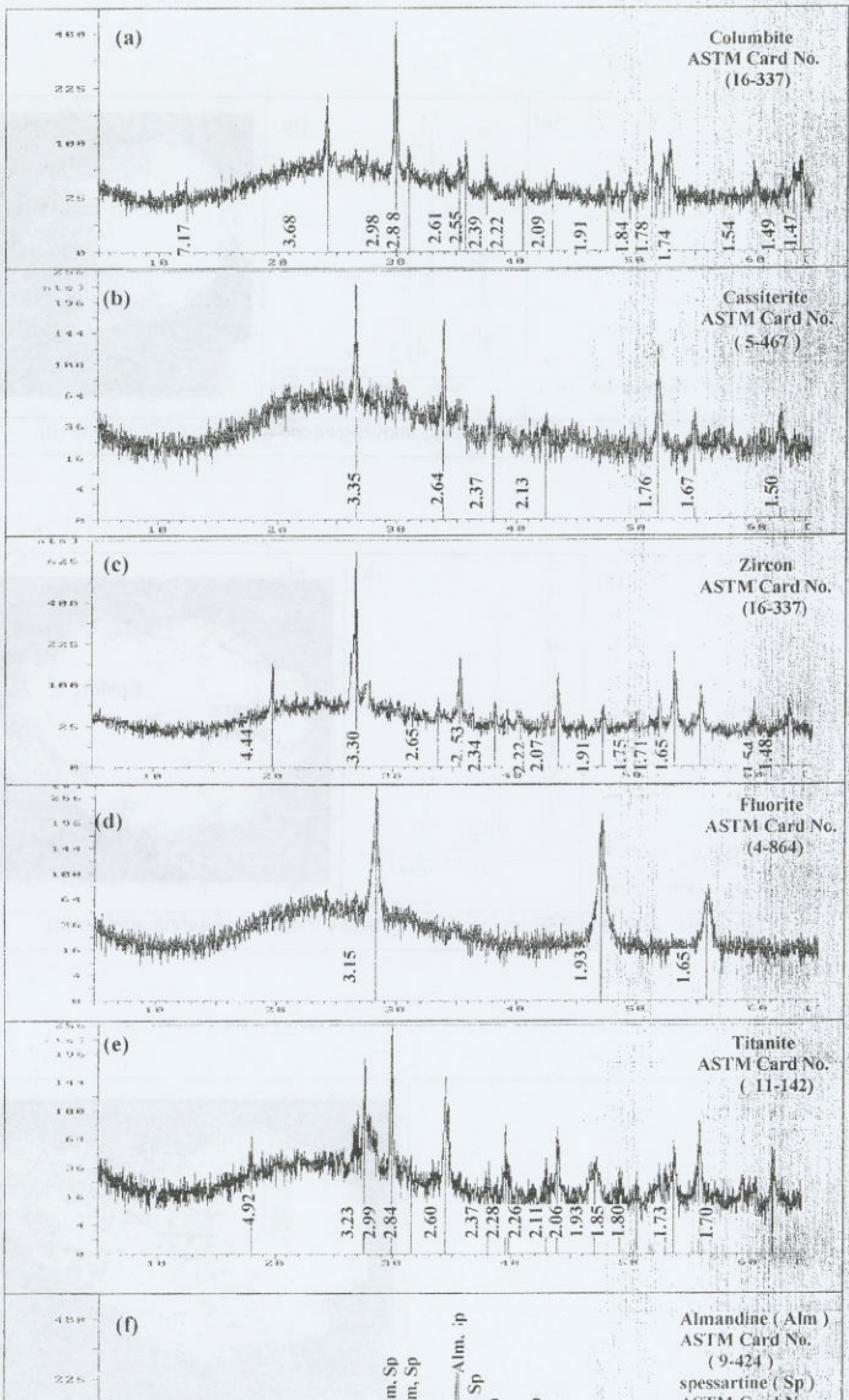

Fig. (28): X-ray diffractograms of recorded minerals from albitized granites of Nuweibi area.
(a) Columbite (b) Cassiterite (c) Zircon (d) Fluorite (e) Titanite (F) Garnet

Geochemical characteristics of Nuweibi albitized granites

Eight representative rock samples from Nuweibi granite have been chemically analyzed for major oxides and trace elements. The chemical analyses data are given in table (3). The average chemical composition of the studied albitized granite is closely similar to the average contents of albitized granite reported by Geological Survey of Egypt (1974); Sabet *et al.*, (1976), Arslan (1997), Ali (2003), Zaki (2007) and Abdalla *et al.*, (2008).

Table (3): Major oxides (wt %), trace element (ppm) contents and CIPW Norms of Nuweibi albitized granite.

Major Oxides	1	2	3	4	5	6	7	8	Av.
SiO_2	73.21	72.89	73.76	72.58	72.45	72.47	72.95	72.26	72.82
TiO_2	00.23	00.20	00.23	00.20	00.19	00.20	00.23	00.22	00.21
Al_2O_3	14.25	14.80	14.07	14.51	14.00	13.81	13.89	13.98	14.16
Fe_2O_3	00.37	00.42	00.50	00.28	00.65	00.60	00.67	00.53	0.50
FeO	00.33	00.41	00.59	00.31	00.66	00.70	00.58	00.63	0.53
MnO	00.05	00.06	00.05	00.06	00.07	00.09	00.06	00.05	0.06
MgO	00.31	00.32	00.28	00.38	00.38	00.40	00.35	00.24	0.38
CaO	01.65	01.00	01.09	01.20	01.70	01.73	01.79	01.12	1.41
Na_2O	05.57	05.61	05.12	05.85	05.53	05.84	05.56	06.00	5.63
K_2O	02.78	03.15	03.08	03.75	03.13	03.04	03.02	03.73	3.21
P_2O_5	00.13	00.09	00.13	00.15	00.12	00.13	00.14	00.12	0.13
L.O.I	01.00	00.92	00.98	00.64	00.92	00.80	00.67	01.00	0.86
Total	99.88	99.87	99.88	99.91	99.80	99.81	99.90	99.88	99.87
Qz	26.79	25.62	29.46	21.93	35.81	23.64	25.74	21.34	
Or	16.64	18.84	18.49	22.35	18.53	18.25	18.02	22.26	
Ab	47.13	47.47	43.32	49.50	29.87	49.41	47.04	50.77	
				Trace elements (ppm)					
Zn	69	101	182	40	60	97	143	144	104.5
Zr	147	151	164	150	147	151	133	153	149.5
Rb	547	595	763	477	584	753	615	694	628.5
Y	73	75	101	67	24	95	90	103	78.5
Ba	43	25	24	32	20	20	14	16	24.25
Pb	22	20	56	30	19	48	25	28	31.00
Sr	18	13	10	18	63	17	10	9	19.75
Ga	83	92	58	98	62	94	87	60	79.25
Nb	58	66	51	47	61	55	43	79	57.5

According to Raguin (1976) and Nockolds *et al.* (1979), granites are modified to varying extent by the action of residual fluids rich in water and hence these rocks undergo deuteric and hydrothermal alterations. Due to the albitized granites just altered rocks, therefore specialist diagrams concerning with different types of hydrothermal alterations can be applied. Firstly, the normative Qz- Ab-Or of Stemprok (1979) in which the altered granitic samples could be revealed the metasomatic trends such as sodic, potassic, silicic and greisens (Fig.29a). Secondly, Q-P diagram of Debon and Le Fort (1983) where, P= K-Na and Q= Si/3-(K-Na). This diagram used to differentiate between different hydrothermal alteration trends; pointed out the samples with high negative P parameter may correspond to the hydrothermally altered rocks (Fig. 29 b). Thirdly, Na%-K% variation diagram of Cuney *et al.* (1989) shows different alteration trends (Figs. 29 c).

Accordingly, Nuweibi albitized granites exhibit sodic characters, and may underwent an extensive hydrothermal alteration mainly Na-metasomatism, they contain conspicuous enrichment of Na_2O (Na_2O vary from 5.12 to 6.0 % with an average of about 5.64%). The presence of albite is the most pronounced features of metasomatic alteration (albitization) in Nuweibi granites. During albitization Na and Al has been enriched while losses in K, Si, and leaching in U and REE were occurred during the emplacement of the andesite dykes (the source of heat supply). Consequently, the metasomatic replacements of feldspars into albite will occurred (Laves and Soldates, 1965). This process is generally compatible with the petrographic examination of the studied granites where discrete laths of albite are developed along potash feldspar boundaries.

Fig. (29): Hydrothermal alteration diagrams

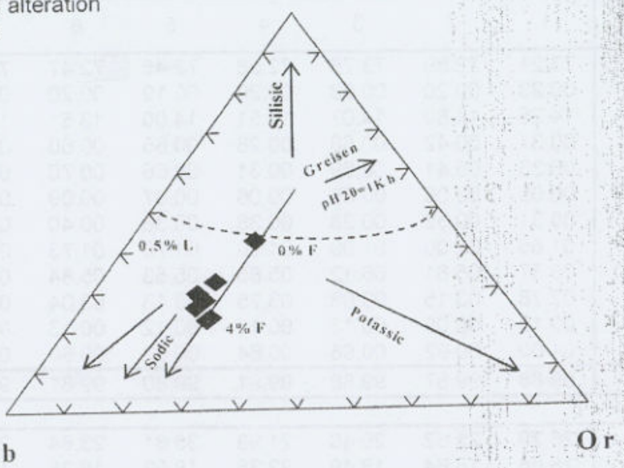

Fig.(29 a): Normative Qz-Ab-Or (Stemprok, 1979)

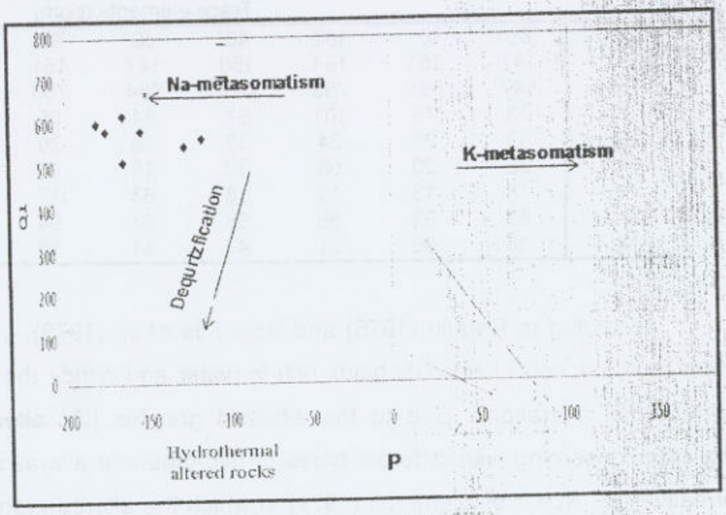

Fig. (29 b): Q-P diagram (Debon and Le Fort, 1983)

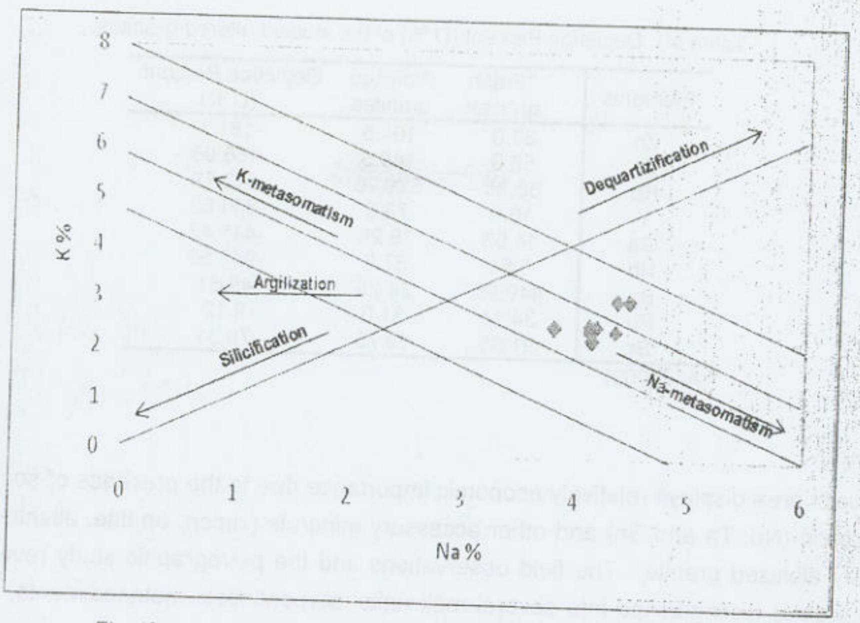

Fig. (29c): Na%-K% hydrothermal alteration diagram
(Cuney *et al.* 1989)

Additionally, the study of the trace elements in the granitic bodies and related altered zones should yield useful information on rock/fluid interaction characteristics as well as the physicochemical features of the system. Thus, the geochemical behavior of trace elements during the alteration can be evaluated using the depletion percent (D %) equation (Dawoud *et al.*, 2000). Consequently, the Nuweibi altered granites normalize to its corresponding fresh granite, mainly muscovite-biotite granites (Gabal Humr adjacent to Gabal Nuweibi in Nuweibi area) that given by Ali (2003).

$$D\ \% = [(C_f - C_w) / C_f]*100$$

Where, C_f: is the concentration of an element in the corresponding fresh granite sample

C_w: is the concentration of this element in the equivalent altered granite sample. The depletion percent (D %) of the trace elements in the altered samples was shown in table (4). The negative value of the D % for an element indicates enrichment of the element by alteration and vice versa.

Accordingly, Nuweibi albitized granites exhibit significant enrichment in Zr, Zn, Y, Rb, Ga and Nb that could be attributed to the existence of some resistant minerals such as zircon, monazite and columbite which causing the concentration of these elements in the altered rocks. In addition to, the elements Zr, Y and Ga belong to so called high field strength elements that are essentially immobile and resistance to weathering (Middelburg *et al.*, 1988).

Knowing that the expected decrease in Rb content with decreasing of K content in the albitized granites, the observed enrichment of Rb in the studied rocks (Rb vary from 449 to 763 ppm; Av.=590 ppm), is likely attributed to that Rb concentration increases in liquids rich in volatile component, being concentrated during the late magmatic differentiation (Ekwere, 1985). On the otherhand, the elements Sr, Ba and Pb exhibiting a marked decrease in the altered samples rather than the fresh ones. Ba depletion may be related to K-depletion during Na-metasomatism due to substitution of K by Na. Generally, Sr, Ba and Rb decrease as albitization increases (Neiva, 1974).

Table (4): Depletion Percent (D %) of the studied altered granites

Elements	*Fresh granites	Albitized granites	Depletion Percent (D %)
Zn	37.0	104.5	-181.1
Zr	56.0	149.5	-166.96
Rb	88.35	629.75	-612.79
Y	16.0	78.5	-390.62
Ga	14.53	79.25	-445.42
Nb	5.51	57.5	-943.56
Ba	449.95	24.25	49.61
Pb	34.11	31.0	9.12
Sr	91.05	19.75	78.31

* Ali (2003)

Conclusion

Nuweibi area displays relatively economic importance due to the presence of some rare metal mineralization (Nb, Ta and Sn) and other accessory minerals (zircon, apatite, allanite and fluorite) at Nuweibi albitized granite. The field observations and the petrographic study revealed that the mapped area is distinguished into several rock units: serpentinites, metasediments, metagabbros and older granites that intruded by albitized granites

Radiometically, the studied rocks encountered (metasediments, serpentinites, metagabbros and older granites) exhibits low radioactivity levels while the albitized granites can be attain relatively moderate eU and eTh contents. The eU contents vary from 7 to17 ppm with an average of 10 ppm while eTh contents range from 13 to 26 ppm with an average of 20 ppm. The western part of Nuweibi granites generally exhibits distinctly high radioactive level than do other parts. The post-magmatic processes played a major role in uranium enrichment in studied albitized granites.

The radioactivity of Nuweibi albitized granites may be attributed to the dominance of thorium and thorium bearing minerals as monazite and uranothorite. Moreover, very scarcely grains of secondary uranium minerals as uranophane, autunite and chernikovite are recorded. Furthermore, zircon was documented as free grains or as inclusions within crystal lattice of cassiterite, garnet and titanite. Also, the EDX microanalysis revealed the presence of REE signature in some recorded minerals such as allanite, fluorite, apatite, chevkinite and manganocoltan. On the other hand, tantalite, columbite, tapiolite, and cassiterite are dominant as a rare-metal mineralization (Nb, Ta & Sn).

The taxopiokilitic texture as well as the prismatic bipyramidal zircon is strong evidence for the magmatic origin of Nuweibi granite. Unlike the albitization processes give an idea about the Nuweibi granite may have been underwent an extensive hydrothermal alteration discriminated by Na-metasomatism. In addition to, the presence of characteristic variety of zircon such as mud zircon, as well as hydrothermal mineral (columbite, cassiterite, garnet, fluorite and apatite) confirming the multistage of hydrothermal metasomatic origin. On the other hand, Nuweibi albitized granites display negative depletion percent (D %) values indicate enrichment of Zr, Rb, Y, Ga, Nb and Zn by alteration that could be attributed to the existence of some resistant and economic heavy minerals in the study area. while Ba, Sr and Pb show positive depletion percent (D %) values indicate their depletion during alteration.

Acknowledgments

The author wishes to express his deep thanks and gratitude to Prof. M. E. Ibrahim head of research sector, Prof. F.S. Bakhit, Prof. A.A. Abd El Wahed and Prof. A.M. Dardier, Nuclear Materials Authority, Egypt for their sincere reviewing, constructive criticism and fruitful comments, during the earlier version of this paper.

References

Abdalla, H. M., Helba, H. and Mohamed, F.H. (1998) Chemistry of columbite-tantalite minerals in rare metal granitoids, Eastern Desert, Egypt. Minerals. Mag., 62, 821-836.

Abdalla, H. M. and Mohamed, F.H. (1999) Mineralogical and geochemical investigation of emerald and beryl mineralization, Pan-African belt of Egypt: Genetic and exploration aspects. J. Afr. Earth Sci., 28,581-598.

Abdalla, H. M., Helba, H. and Matsueda, H. (2008) Chemistry of zircon in rare metal granetoids and the associated rocks, Eastern Desert, Egypt. Resource geology, 59, No.1, 51-68.

Abdalla, H. M., Matsueda, H., Obeid, M. A. and Takahshi, H. (2008) Chemistry of cassiterite in rare metal granetoids and the associated rocks in the Eastern Desert, Egypt. J. of mineralogical and petrological Sci. 103, 318-326.

Abdel-Wahed, M. A. (2004) Structural and metamorphic evaluation of Wadi Dubur metasediments, Central Eastern Desert, Egypt. Ann. Geol. Surv. Egypt, 26, 71-105.

Abu-El Maaty, M. A. and Khalil, M. M. (1999 a) Mineral chemistry as a guide to magmatic evaluation of some basement rocks from Nuweibi area, Central Eastern Desert, Egypt. Ann. Geol. Surv. Egypt, Cairo, Egypt, 22, 287-307.

Abu-El Maaty, M. A. and Khalil, M. M. (1999 b) Petrography and geochemistry of some plutonic rocks of Nuweibi and Mueilha areas, Central Eastern Desert, Egypt. J. Miner. Soc. Egypt, Cairo, 11, 63-89.

Abu-El Maaty, M. A. and Ali Bik M. W. (2000) Petrology of alkali feldspar granites of Nuweibi and Gabal El-Mueilha, Central Eastern Desert. Egypt J. geol. Soc. Egypt, Cairo, 44, No. 1, 2000, 127-148.

Aero Service (1984) Final operations report of airborne magnetic/radiation survey in the Eastern Desert. Work completed for the Egyptian General Petroleum Corporation (EGPC). Aero Service, Houston, Texas. April 1984, Six Volumes.

Ali, K.G. (2003) Geology and radioactivity of Naba-Nuweibi area, Central Eastern Desert, Egypt. Ph.D Thesis, Fac.Sci. Ain Shams Univ.194P.

Amin, M.S., Mansour, M.S., Kabesh, M.L.A. and El-Far, D.M. (1952) Geology of the Naba district. Geol. Surv. Egypt.

Arslan, A. I., Helba, H. A., Khalil, S.O., Morteani, G. (1997) Bedrock geochemical prospecting and ore potentiality of the rare metal-bearing granite at Nuweibi area, Eastern Desert, Egypt. Third Conf. on geochem. Fac. Sci. Alex. Egypt, 375-388.

Awad, WK. (1973) Application of geophysical methods for mineral prospecting at Abu-Dabbab Nuweibi areas, Central Eastern Desert of Egypt, M. Sc. Thesis, Geol. Fac.Sci. Cairo Univ. Cairo, Egypt, Abstr., 63P.

Cambon, A.R. (1994) " Uranium deposits in granitic rocks: notes. The National Training Coarse on Uranium Geology and Exploration organized by IAEA and NMA on 8-20 Jan 1994, Egypt.

Cuney, M., Leorty, J., Valdiviezo, P. A., Daziano, C., Gamba, M., Zarco, J., Morello, O., Ninci, C. and Molina, P. (1989) Geochemistry of the uranium mineralized Achala Granitic Complex, Argentina: comparison with Hercynian peraluminous leucogranites of Western Europe. Metallogensis of Uuranium Deposits, IAEA-Tc-452/6, Vienna. 211-232.

Debon, F. and Le Fort, P. (1983) Chemical-mineralogical classification of the common plutonic rocks and associations. Trans. R. Soc. Edinburgh (Earth Science), 73,135-149.

Dewed, M., Eliwa, H. A. and Attia, M. S., (2000) On the behavior of the rare earth and other trace elements during the weathering of some granitic rocks, Eastern Desert, Egypt. Ann. Geol. Surv. Egypt, V.XXIII, 291-302.

Egyptian Geological Survey (1974) Mineral deposits in Egypt. Geol. Surv. Egypt. Pap. No.61,19-26.

Egyptian Geological Survey (1991)Basement rocks of Mersa Alam Quadrangle, Egypt. Scale, 1:100,000

Ekwere, S. J. (1985) Li, F and Rb contents and Ba/Rb and Rb/Sr ratio as indicators of postmagmatic alteration and mineralizartion in the granitic rocks of the Banke and Ririwai younger granite complexes, Northern Nigeria. Mineral. Deposita, 20, 89-93.

El Gemmizi, M.A. (1984) On the occurrence and genesis of mud zircon in the radioactive psammitic gneiss of Wadi Nugrus, Eastern Desert, Egypt,J.Univ.Kuwait, Sci., 11, 285-293.

El-Kammar, A.A., El-Hazik, N.T., Mahdi, M. and Ali, N. (1997) Geochemistry of accessory minerals associated with radioactive mineralization in the Central Eastern Desert, Egypt. J. Afr. Earth Sci, 25(2), 237-252.

El-Tabbal, H.K.,(1980) Mineralogical studies on some rare-metal apograintes from Nuweibi and Abu Dabbab areas, Eastern Desert, M. Sc. Thesis, Fac. Sci., Al Azhar Univ., Cairo, Egypt.

Ghoneim, M., (2003) Mineralization of niobium and tantalum in the Central Eastern Desert, Egypt, UAR. 8th Arab Conf. on mineral resources, Sana'a, Yemen, 13-16, Oct. 2003, 1,121-127.

Helba, H. A., Trumbull, R.B., Morteani, G., Khalil, S.O. and Arslan, A. I. (1997) Geochemical and petrographic studies of Ta mineralization in the Nuweibi albite granite complex, Eastern Desert, Egypt. Mineral, Deposita, 32,164-179.

Kamel, O.A., El-Tabbal, H.K. (1980) Petrology and mineralogy of Nuweibi and Abu-Dabbab rare metal apogranites, Eastern Desert, Egypt. Accademia National dei lincel Atti del Convegni Lincei, 47, 685-705.

Kraus, H.E., Hunt, F.W. and Ramsdell, S.L.(1951) An introduction to the study of minerals and crystals, by the mcgraw-Hill Book company Inc.292p.

Laves, F. and Soldatos, K. (1965) "Die albite-Mikroklin orienticurung nezich vugen in micrklin perthiten und devegenetische deutung".Z. Krist., 118, 69-102.

Middelburg, J.,Van Der Weijden, C. H. and Woittiez, J. R. W., (1988) Chemical processes affecting the mobility of major, minor and trace elements during weathering of granitic rocks. Chem. Geol., 68, 253-273.

Naim, G. M., El-Miligy, A.T. and Soliman, K. (1996) Tantalum-niobium-tin mineralization in Central Eastern Desert of Egypt. Proc. Egypt, Geol. Surv. Centennial Conf. (1896-1996), Cairo, Nov. 1996, Spec. Pupl. Pap. No. 75, 599-622.

Neiva, A. M. R. (1974) Greisenization of muscovite-biotite albite granite of northern Portugal, chemical geology, 13, Issue 4, 295-308

Nockolds, S. R., Knox, R.W., O. B., Chinner, G. A. (1979) Petrography for students. Great Bretain, Fakenham Press, Norfolk, 427p.

Raguin, E. (1976) Geologie du granite. Paris, New York, Barcelone, Milan, 275p.

Riad, A.M. (1979) Geology and petrology on some apogranite occurrences, Nuweibi area, Eastern Desert, Egypt,. M Sc.Thesis, Geol. Fac. Sci., Al Azhar Univ. Cairo, Egypt, Abstr, 140 p.

Sabet, A.H., and Tsogoev, V. (1973) Problems of geological and economic evaluation of tantalum deposits in apogranites during stages of prospecting and exploration. Geol. Surv. Egypt, Cairo, Egypt, Ann. 3, 87-107.

Sabet, A.H., Chbanenko, V., and Tsogoev, V. (1973) Tin, Tungsten and rare metal mineralization in the Central Eastern Desert of Egypt. Geol. Surv. Egypt. Cairo, Egypt, Ann. 3, 75-86.

Sabet, A.H., Tsogoev, V.B., Shibanin, S.P., El-Kadi, M.B. and Awad, S. (1976) The placer tin deposits of Abu-Dabbab, Igla and Nuweibi. Ann. Geolgy Surv. Egypt, Cairo, Egypt, 6, 169-180.

Sabet, A.H., (1980) Tin-rare metal deposits at Abu-Dabbab and Nuweibi, Eastern Desert, Egypt. Geol. Surv. Egypt, Rep. Cairo, Egypt, 38 p.

Severov, E.A. (1963) Concerning the genesis of Niobium-containing granites. Crystallochemistry of rare elements of the Academy of Sciences of the U.S.S.R., Moscow, 5, Issue 12, 1623 - 1630

Shapiro, L. and Brannock, W. W. (1962) Rapid analysis of silicate, carbonate and phosphate rocks. U. S. Geol. Surv. Bull. 1144A, 56p.

Stemprok, M. (1979) Mineralized granites and their origin. Episodes, 3, 20-24.

Zaki, M. A. E. (2007) Study of the relation between albite-enrichment and u-anomalies in Um Naggat and Abu Dabbab granitic bodied, Eastern Desert, Egypt. M. Sc. Thesis, Fac. Sci. Benha Univ., Egypt.

الطواهرالمعدنية والجيوكيميائية والأشعاعية لصخور القاعدة بمنطقة نويبع
وسط الصحراء الشرقية - مصر.

صلاح صبحى البلاقصى * محمد أحمد وتيت سامح محمد منصور
هيئة المواد النووية ص.ب 530 المعادى- القطامية * قسم الجيولوجا-كلية العلوم- جامعه بنها

يتناول البحث دراسة الظواهر المعدنية والجيوكيميائة والأشعاعية لصخورالجرانيت المؤلبت بمنطقة نويبع فى وسط الصحراء الشرقية مصر تهدف التعرف على محتواها المعدنى والأشعاعى وعلاقتها بالتحولات المختلفة. اتضح من الدراسات الحقلية والبتروجرافية أن منطقة الدراسة تتكون من صحور السربنتين والصخور الرسوبية المتحولة والميتاجابرو والجرانيت القديم والجرانيت المؤلبت.

اثبتت الدراسات الراديومترية أن صخور المنطقة ذات أشعاعية ضعيفة بينما صخور الجرانيت المؤلبت ذات محتوي اشعاعي متوسط وخاصة الجزء الغربي. ترجع أشعاعية الجرانيت المؤلبت لوجود بعض المعادن مثل الثوريت واليورانوثوريت والمونازيت وكذلك معادن اليورانيوم الثانوية نادرة الوجود مثل اليورانوفين والأوتونيت والشرنوكوفيت بالأضافة الى معدن الزركون الذى يتواجد كحبيبات مفردة أو متداخل مع معادن أخرى مثل الكاستريت والجارنت والتيتانيت. وقد سجلت الدراسة تواجد بعض المعادن الحاملة للعناصر النادرة مثل الألنيت والشفكنيت والفلوريت والأباتيت.بالأضافة الى وجود بعض المعادن الحاملة للفلزات النادرة (Nb, Ta & Sn) مثل الكولومبيت والتانتاليت والتابيوليت والكولتان والكاستريت والأتاكاميت والأبيدوت.

توجد بعض الأدلة لتكون الجرانيت الحديث مجمانيا مثل وجود (Taxopiokilitic texture) وكذلك انواع مميزة من الزركون (Prismatic bipyramidal zircon) ثم خضع هذا الجرانيت لمراحل عديدة لتأثير المحاليل المائية الحارة نتج عنة عملية الألبتة (Na-metasomatism) حيث تغلب الصفة الصودية والتحول الصودى بالأضافة لوجود انواع مميزة من الزركون (Mud zircon) وكذلك وجود بعض من المعادن المائية الحارة مثل الكاستريت والجاربت والأباتيت والفلوريت. وقد حدث اثراء لبعض من العناصر الشحيحة أثناء عملية التحول مثل Zr, Zn, Rb,Y, Nb & Ga بينما حدث نقص لعناصر أخرى مثل Ba, Sr& Pb . وقد وجد أن عملية الأثراء أو النقص فى العناصر الشحيحة لها أرتباط ببعض المعادن الأقتصادية المتواجدة بالمنطقة.
توجد بعض الأدلة لتكون الجزانيت الحديث مجمانيا مثل وجود (Taxopiokilitic texture) وكذلك انواع مميزة من الزركون (Prismatic bipyramidal zircon) ثم خضع هذا الجرانيت لمراحل عديدة لتأثير المحاليل المائية الحارة نتج عنة عملية الألبتة (Na-metasomatism) حيث تغلب الصفة الصودية والتحول الصودى بالأضافة لوجود انواع مميزة من الزركون (Mud zircon) وكذلك وجود بعض من المعادن المائية الحارة مثل الكاستريت والجاربت والأباتيت والفلوريت. وقد حدث اثراء لبعض من العناصر الشحيحة أثناء عملية التحول مثل Zr, Zn, Rb,Y, Nb & Ga بينما حدث نقص لعناصر أخرى مثل Ba, Sr& Pb . وقد وجد أن عملية الأثراء أو النقص فى العناصر الشحيحة لها أرتباط ببعض المعادن الأقتصادية المتواجدة بالمنطقة.